J|A|C|S
ARTICLES
Published on Web 01/03/2007

Engineering Copper Sites in Proteins: Loops Confer Native Structures and Properties to Chimeric Cupredoxins

Chan Li, Mark J. Banfield, and Christopher Dennison*

Contribution from the Institute for Cell and Molecular Biosciences, Medical School, Newcastle University, Newcastle upon Tyne NE2 4HH, United Kingdom

Received August 24, 2006; E-mail: christopher.dennison@ncl.ac.uk

Abstract: The ligand-containing loops of two copper-binding electron-transfer proteins (cupredoxins) have been swapped. In the azurin (AZ) variant in which the plastocyanin (PC) sequence is introduced (AZPC), the loop adopts a conformation identical to that in PC. The reduction potential of AZPC is raised as compared to AZ and matches that of PC. In the previously published AZAMI variant (AMI = amicyanin), the shorter introduced loop adopts the same conformation as in AMI, and the reduction potential is lowered to equal that of AMI (Yanagisawa, S.; Dennison, C. *J. Am. Chem. Soc.* **2004**, *126*, 15711−15719. Li, C.; et al. *Proc. Natl. Acad. Sci. U.S.A.* **2006**, *103*, 7258−7263). Thus, the loop structure plays an important role in tuning the reduction potential of a type 1 copper site with contributions from protein dipoles in this region probably the most important feature. The structure of the loop also seems to be a major factor in controlling dissociation and protonation of the C-terminal His ligand, which can act as a switch to regulate electron-transfer reactivity. The PCAZ variant (PC with the AZ loop) possesses an active site, which is different from those of both PC and AZ, and it is assumed that the introduced loop does not adopt a structure as in AZ. This contributes to the observed instability of PCAZ and highlights that loop−scaffold interactions are important for stabilizing the active site of a cupredoxin.

Biological electron-transfer (ET) copper sites have a rigid β-barrel cupredoxin scaffold onto which a type 1 (T1) copper binding loop is grafted.[1−3] The length and composition of this loop, which contains coordinating His, Cys, and usually Met residues, varies (see Figure 1) in analogues with distinct functional roles, that is, which interact with different partners and have altered reduction potentials.[3−11] This loop must therefore be important for tuning physiological properties but cannot vary too drastically or the delicate balance between the Cu(II) and Cu(I) sites that ensures minimal changes upon redox interconversion[12] will be compromised. To truly appreciate this subtlety of metalloprotein structure, variants in which active site loops have been replaced with naturally occurring sequences from other cupredoxins with different functional properties have been prepared[3,9,13−17] to assess the importance of this feature for structure and reactivity. Despite all of these loop-directed mutagenesis studies, very few structures of the chimeric products have been determined. The structure of the azurin (AZ) variant into which the shortest naturally occurring T1 sequence from amicyanin (AMI) has been introduced (see Figure 1) demonstrates that the loop adopts a conformation almost identical to that found in AMI.[9] This homology extends to the hydrogen-bonding arrangement around the active site, and even to certain solvent molecules in the vicinity of the copper ion. However, the Cu(II) site structure of this AZAMI variant is almost identical to that of AZ (the cupredoxin whose scaffold has been used), which is different from that in AMI (see Figure 1). Nevertheless, the reduction potential (E_m value) of AZAMI is lower than that of AZ, with a value almost identical to that of AMI. The short AMI loop is highly constrained, with a Pro residue either side of the central His ligand. To determine if the loop is really able to confer its structure onto a particular scaffold and fine-tune reactivity, we have introduced the corresponding region from plastocyanin (PC) into AZ (see Figure 1). The loops of these two cupredoxins, although similar in length, have very different sequences and conformations. The structure and properties of AZPC confirm that the ligand-containing loop does play a major role in tuning important

(1) Adman, E. T. *Adv. Protein Chem.* **1991**, *42*, 144−197.
(2) Dennison, C. *Coord. Chem. Rev.* **2005**, *249*, 3025−3054.
(3) Dennison, C. *Dalton Trans.* **2005**, 3436−3442.
(4) Nar, H.; Messerschmidt, A.; Huber, R.; van de Kamp, M.; Canters, G. W. *J. Mol. Biol.* **1991**, *221*, 765−772.
(5) Crane, B. R.; Di Bilio, A. J.; Winkler, J. R.; Gray, H. B. *J. Am. Chem. Soc.* **2001**, *123*, 11623−11631.
(6) Xhu, Y.; Ökvist, M.; Hansson, Ö.; Young, S. *Protein Sci.* **1998**, *7*, 2099−2105.
(7) Guss, J. M.; Freeman, H. C. *J. Mol. Biol.* **1983**, *169*, 521−563.
(8) Cunane, L. M.; Chen, Z. W.; Durley, R. C. E.; Mathews, F. S. *Acta Crystallogr., Sect. D: Biol. Crystallogr.* **1996**, *52*, 676−686.
(9) Li, C.; Yanagisawa, S.; Martins, B. M.; Messerschmidt, A.; Banfield, M. J.; Dennison, C. *Proc. Natl. Acad. Sci. U.S.A.* **2006**, *103*, 7258−7263.
(10) Baker, E. N. *J. Mol. Biol.* **1988**, *203*, 1071−1095.
(11) Romero, A.; Nar, H.; Huber, R.; Messerschmidt, A.; Kalverda, A. P.; Canters, G. W.; Durley, R.; Mathews, F. S. *J. Mol. Biol.* **1994**, *236*, 1196−1211.
(12) Gray, H. B.; Malmström, B. G.; Williams, R. J. P. *J. Biol. Inorg. Chem.* **2000**, *5*, 551−559.
(13) Dennison, C.; Vijgenboom, E.; Hagen, W. R.; Canters, G. W. *J. Am. Chem. Soc.* **1996**, *118*, 7406−7407.
(14) Buning, C.; Canters, G. W.; Comba, P.; Dennison, C.; Jeuken, L.; Melter, M.; Sanders-Loehr, J. *J. Am. Chem. Soc.* **2000**, *122*, 204−211.
(15) Remenyi, R.; Jeuken, L. J. C.; Comba, P.; Canters, G. W. *J. Biol. Inorg. Chem.* **2001**, *6*, 23−26.
(16) Yanagisawa, S.; Dennison, C. *J. Am. Chem. Soc.* **2003**, *125*, 4974−4975.
(17) Yanagisawa, S.; Dennison, C. *J. Am. Chem. Soc.* **2004**, *126*, 15711−15719.

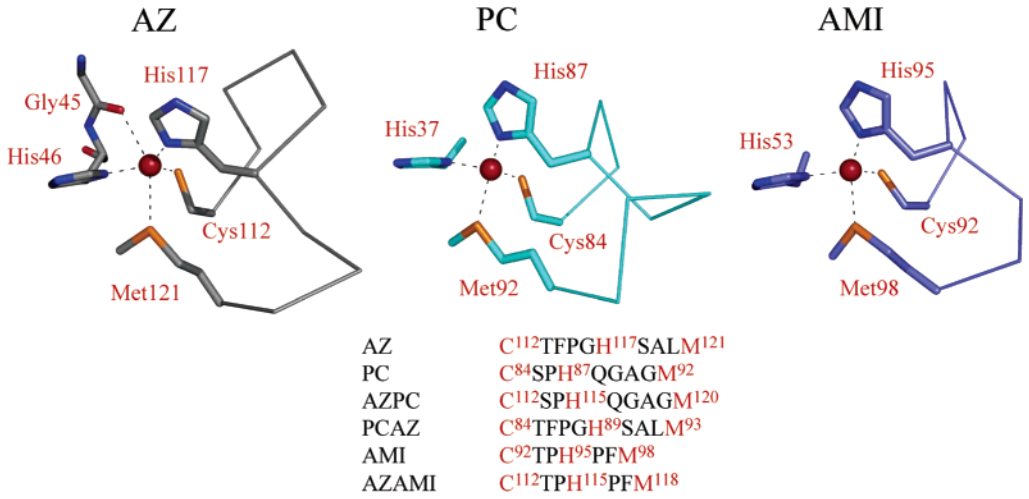

Figure 1. Representations of the active site structures (prepared using Pymol) of *Pseudomonas aeruginosa* azurin (AZ),[4,5] plastocyanin (PC) from spinach,[6] and *Paracoccus denitrificans* amicyanin (AMI)[8] highlighting the different structures of their ligand-containing loops. Also shown are the loop sequences of these proteins along with those of the AZPC (AZ scaffold with PC loop), PCAZ (PC scaffold with AZ loop), and AZAMI (AZ scaffold with AMI loop) variants.[9] The copper ion is shown as a red sphere, and the ligands are numbered.

physiological features of this family of metalloproteins. To test if this conclusion is applicable to all cupredoxins, we have also prepared the PC variant into which the AZ loop has been introduced (PCAZ). In this case, the chimeric molecule is unstable in solution and could not be characterized to the same degree as AZPC. The loop−scaffold interface in cupredoxins can be disrupted by extensive loop-directed mutations.

Materials and Methods

Loop Mutagenesis. Loop mutagenesis was carried out using the QuikChange (Stratagene) site-directed mutagenesis kit. The Cys^{112} to Met^{121} loop of *Pseudomonas aeruginosa* azurin (AZ) was mutated from $C^{112}TFPGH^{117}SALM^{121}$ to $C^{112}SPH^{115}QGAGM^{120}$ with the primers catgttcttctgcagcccgcatcagggcgcgggcatgaagggcacc (forward) and ggtgcccttcatgcccgcgccctgatgcgggctgcagaagaacatg (reverse) using pTrcAZ, a pTrc99a derivative harboring the gene for AZ including the signal peptide, as the template.[17] This introduces the C-terminal ligand-containing loop of a typical higher plant (such as spinach or poplar) plastocyanin (PC) into AZ and is thus termed AZPC. The Cys^{84} to Met^{92} loop of spinach PC was mutated from $C^{84}SPH^{87}QGAGM^{92}$ to $C^{84}TFPGH^{89}SALM^{93}$ (the AZ loop sequence) using the primers caagttctactgcacctttccgggccatagcgcgctgatggtgggaaaag (forward) and cttttcccaccatcagcgcgctatggcccggaaaggtgcagtagaacttg (reverse) along with pTrcPC, a pTrc99a derivative harboring the gene for spinach PC including the AZ signal peptide,[17] as the template to give PCAZ. Both strands of the mutated plasmids (pTrcAZPC and pTrcPCAZ) were sequenced to verify the changes made.

Cell Growth, Protein Isolation, and Purification for AZPC. *Escherichia coli* JM101 harboring pTrcAZPC was grown, cells were harvested 5 h after induction, and the periplasmic proteins were obtained as described previously.[17] The isolation and purification of AZPC were carried out as described before[17] except that the protein was fully oxidized before loading onto the third diethylaminoethyl (DEAE) sepharose column. A Resource Q column (GE Healthcare) was used to separate the Cu(I) variant (reduced using 2 mol equiv of ascorbate) from a colorless impurity, which was most probably Zn(II) protein.[18] This column was equilibrated in 1 mM Tris pH 9.0, and the protein eluted with a gradient of 0−100 mM NaCl in the same buffer. Pure oxidized AZPC with an A_{280}/A_{608} ratio of ≤1.9 gave a single band on a 15% SDS-PAGE gel. The final yield of AZPC was ∼12 mg/L of cell culture.

Cell Growth, Protein Isolation, and Purification for PCAZ. *Escherichia coli* TG1 (pTrcPCAZ) was grown, cells were harvested 5 h after induction, and the periplasmic proteins were obtained as described previously.[17] The PCAZ-containing solution was incubated with (diethylamino)ethyl (DEAE) sepharose (GE Healthcare) material for 60 min at 4 °C with stirring. The bound proteins were eluted with 10 mM tris(hydroxymethyl)aminomethane (Tris) at pH 8.0 with a NaCl gradient from 0 to 300 mM. The PCAZ fractions were exchanged into 10 mM Tris pH 7.2 and loaded onto a HiTrapQ column (GE Healthcare) and eluted with a 0−250 mM NaCl gradient in the same buffer. The PCAZ fractions were exchanged into 20 mM Tris pH 8.0 plus 200 mM NaCl and loaded onto a Superdex 75 (GE Healthcare) gel filtration column and eluted with the same buffer. Pure oxidized PCAZ (∼0.8 mg/L of cell culture) with an A_{278}/A_{608} ratio of ≤1.6 gave a single band on a 15% SDS-PAGE gel.

UV/Vis Spectrophotometry. Ultraviolet/visible (UV/vis) spectra were measured at 25 °C on a Perkin-Elmer λ 35 spectrophotometer with the proteins in 20 mM Tris pH 8.0.

Metal Concentration Determinations and the Molecular Weights of AZPC and PCAZ. The concentration of copper and zinc in samples of AZPC and PCAZ in 10 and 2 mM Tris pH 8.0, respectively, was determined using a Thermo Electron Corp. (Cambridge) M Series atomic absorption spectrometer (AAS) as described previously.[9] The molecular weights of AZPC and PCAZ were determined by matrix-assisted laser desorption ionization time-of-flight mass spectrometry (MALDI-TOF MS).

EPR Spectroscopy. X-band electron paramagnetic resonance (EPR) spectra were recorded at −196 °C on a Bruker EMX spectrometer with the protein (2 mM) in 25 mM Hepes pH 7.6 plus 40% glycerol. A sample of diphenylpicrylhydrazyl (DPPH) was used as an external reference, and the program SIMFONIA (Bruker) was used for spectral simulations.

Samples and ^{1}H NMR Spectroscopy of AZPC. AZPC samples for nuclear magnetic resonance (NMR) experiments on the Cu(II), Cu(I), and also on mixtures for ESE rate constant (k_{ese}) determinations and saturation transfer experiments were prepared as described before.[19] Spectra were obtained using standard 1D and WEFT pulse sequences

(18) Nar, H.; Huber, R.; Messerschmidt, A.; Filippou, A. C.; Barth, M.; Jaquinod, M.; van de Kamp, M.; Canters, G. W. *Eur. J. Biochem.* **1992**, *205*, 1123−1129.

(19) Sato, K.; Kohzuma, T.; Dennison, C. *J. Am. Chem. Soc.* **2003**, *125*, 2101−2112.

Table 1. Crystallographic Data Collection, Processing, and Refinement Statistics for AZPC

	Cu(II) pH 5	Cu(I) pH 5	Cu(I) pH 3.5
		Data Collection[a]	
wavelength (Å)	1.542	1.542	1.542
space group	$P2_12_12_1$	$P2_12_12_1$	$P2_12_12_1$
resolution range (Å)	28−1.54 (1.62−1.54)	28−1.6 (1.69−1.6)	36−2.2 (2.32−2.2)
unit cell parameters (Å)	$a = 38.99$, $b = 65.28$, $c = 97.91$	$a = 38.91$, $b = 65.35$, $c = 97.71$	$a = 38.34$, $b = 65.73$, $c = 97.58$
no. of unique reflections	36 537 (4673)	33 470 (4783)	12 989 (1849)
redundancy	4.3 (4.1)	6.7 (6.5)	6.2 (5.8)
$I/\sigma(I)$	19.7 (4.3)	26.6 (5.4)	21.0 (5.4)
completeness (%)	96.6 (86.0)	99.8 (99.0)	99.9 (99.9)
R_{merge} (%)	5.1 (34.1)	5.3 (30.2)	8.1 (34.3)
		Refinement[a]	
resolution	28−1.55 (1.59−1.55)	28−1.6 (1.64−1.6)	36−2.2 (2.26−2.2)
R_{factor} (%)	14.4 (27.1)	14.0 (20.3)	19.9 (26.7)
R_{free} (%)	19.0 (40.1)	18.4 (32.4)	21.9 (31.2)
rmsd bond lengths (Å)	0.018	0.017	0.011
rmsd bond angles (deg)	1.56	1.54	1.289
average *B*-factor (protein − Å^2)	13.4	13.8	19.8
average *B*-factor (ligands − Å^2)	24.5	25.1	21.3

[a] Values in parentheses represent data for the highest resolution shell.

on a Jeol Lambda 500 spectrometer and were processed as described previously.[19] Spin−spin (T_2) relaxation times were derived from peak widths at half-height using the relation $\nu_{1/2} = (\pi T_2)^{-1}$.

Electrochemistry of Proteins. The direct measurement of the E_m values of AZPC and PCAZ was carried out at ambient temperature (22 ± 1 °C) using an electrochemical setup described elsewhere.[20] For AZPC, the pH range studied was 3.6−8.1 using a 1.6 mm diameter gold working electrode modified with 4,4-dithiodipyridine. For PCAZ, data were collected in the pH range 4.4−7.5 using a 1.6 mm diameter pyrolytic graphite working electrode (PGE), which was treated and modified with polylysine and morpholine.[21] Measurements were carried out typically at scan rates of ∼20 mV/s. All reduction potentials (E_m values) were referenced to the normal hydrogen electrode (NHE), and voltammograms were calibrated using the $[Co(phen)_3]^{3+/2+}$ couple (370 mV vs NHE).

Crystallization and Structure Analysis. Cu(II) AZPC was crystallized by the hanging drop method of vapor diffusion at 20 °C using 1.5 μL of protein (15 mg/mL in 5 mM Tris pH 7.5) mixed with 1.5 μL of precipitant solution (0.1 M $MgCl_2$, 29−31% PEG 4000, 0.1 M sodium acetate pH 5.0). Prior to being frozen in a nitrogen stream, the crystals were immersed in a cryo-protectant (5% glycerol, 0.1 M $MgCl_2$, 32% PEG 4000, 0.1 M sodium acetate pH 5.0). A crystal of Cu(II) AZPC was reduced by transferring it to 20 μL of the reservoir buffer containing 10 mM ascorbate. Reduction was considered to be over when the crystal was completely colorless (typically ∼1 h). The reduced crystals were transferred to cryo-buffer containing 10 mM ascorbate prior to being frozen. To enable data collection at pH 4.0 and 3.5, reduced crystals were transferred to reservoir buffer (with 10 mM ascorbate), which had been adjusted to pH 4.0 and 3.5, respectively, and soaked for 5−10 min (if crystals were left for longer periods they started to rapidly deteriorate). Diffraction data were collected at 93 K on a Rigaku Raxis IV^{++} detector with X-rays from a Micromax-007 generator fitted with Osmic "blue" optics. The Cu(II) AZPC structure was solved by molecular replacement using MolRep [as implemented in CCP4][22] and the *P. aeruginosa* Cu(II) AZ structure [PDB entry 4AZU,[4] with the C-terminal ligand-containing loop removed] as a search model. The final Cu(II) AZPC structure was used as a starting model for refinement of the Cu(I) structures. Iterative model building (using Coot)[23] and refinement (Refmac5, as implemented in CCP4) cycles were used to complete the structures of Cu(II) and Cu(I) AZPC. In the final stages of refining the Cu(II) and Cu(I) (at pH 5) structures, anisotropic *B*-factors were refined and hydrogens added at riding positions while monitoring both the R_{factor} and the R_{free}. Detailed data collection, processing, and refinement statistics are given in Table 1. LSQMAN[24] was used to superimpose structures and determine root-mean-square deviations (rmsds) for C^α atoms. Interface areas, defined as the solvent accessible surface area of the free protein minus the accessible surface area of the protein in the homodimers that interact via the region surrounding the exposed C-terminal His ligand, and the percentage of nonpolar atoms in this interface were calculated using a protein−protein interaction server (http://www.biochem.ucl.uk/bsm/PP/server).[25] The solvent accessibility of the active sites (ligands) was calculated with SurfRace[26] using a probe radius of 1.4 Å. The coordinates and structure factors have been submitted to the Protein Data Bank with PDB ID codes 2HX7 [Cu(II) AZPC, pH 5], 2HX8 [Cu(I) AZPC, pH 5], 2HX9 [Cu(I) AZPC, pH 4], and 2HXA [Cu(I) AZPC, pH 3.5].

Results

Molecular Weights of AZPC and PCAZ, AAS Results, and the Stability of PCAZ. The molecular weights of AZPC and PCAZ determined by MALDI-TOF MS are 13 772 and 10 590 Da as compared to theoretical masses of 13 767.6 (with disulfide) and 10 588.9 Da, respectively. Copper concentrations determined by AAS were used to calculate the molar absorptivities (ϵ values) of the ligand to metal charge-transfer (LMCT) bands. Purified AZPC and PCAZ were both found to contain only trace levels of zinc (<2%). Solutions of Cu(II) PCAZ left at 4 °C quickly lose blue color due to reduction. When left for longer periods, the blue color cannot be recovered by oxidation or by the addition of Cu(II). Concomitant with this loss of copper-binding ability is the appearance of a band at around 330 nm in the UV/vis spectrum, which can be associated with oxidation of probably the Cys ligand.[27] This is consistent with

(20) Dennison, C.; Lawler, A. T. P.; Kohzuma, T. *Biochemistry* **2002**, *41*, 552−560.
(21) Battistuzzi, G.; Borsari, M.; Canters, G. W.; de Waal, E.; Leonardi, A.; Renieri, A.; Sola, M. *Biochemistry* **2002**, *41*, 14293−14298.
(22) Collaborative Computational Project, Number 4. *Acta Crystallogr., Sect. D: Biol. Crystallogr.* **1994**, *50*, 760−763.
(23) Emsley, P.; Cowtan, K. *Acta Crystallogr., Sect. D: Biol. Crystallogr.* **2004**, *60*, 2126−2132.
(24) Kleywegt, G. J.; Zou, J. Y.; Kjeldgaard, M.; Jones, T. A. In *International Tables for Crystallography: Crystallography of Biological Macromolecules*; Rossmann, M. G., Arnold, E., Eds.; Kluwer Academic Publishers: Dordrecht, The Netherlands, 2001; pp 353−356, 366−367.
(25) Jones, S.; Thornton, J. M. *Proc. Natl. Acad. Sci. U.S.A.* **1996**, *93*, 13−20.
(26) Tsodikov, O. V.; Record, M. T.; Sergeev, Y. V. *J. Comput. Chem.* **2002**, *23*, 600−609.
(27) van Amsterdam, I. M. C.; Ubbink, M.; van den Bosch, M.; Rotsaert, F.; Sanders-Loehr, J.; Canters, G. W. *J. Biol. Chem.* **2002**, *277*, 44121−44130.

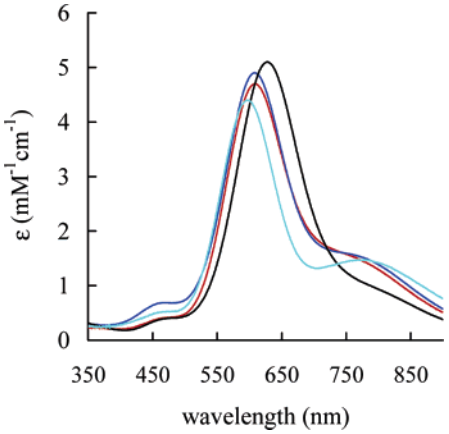

Figure 2. UV/vis spectra of Cu(II) AZPC (red) and PCAZ (dark blue) as compared to those of AZ (black) and PC (cyan) at 25 °C in 20 mM Tris pH 8.0 except for that of AZ, which was obtained with the protein in 10 mM phosphate pH 8.0.

the copper falling out and the Cys ligand becoming modified such that copper can no longer bind. Given the low yield of PCAZ, and its inherent instability, this variant has been characterized in less detail.

UV/Vis Spectra. The UV/vis spectra of AZPC and PCAZ together with those of AZ and PC are shown in Figure 2. The main S(Cys) → Cu(II) LMCT bands for AZPC and PCAZ share a similar position and have comparable intensity. Both features lie approximately mid-way between those for AZ and PC (see Table 2). The spectrum of PCAZ has slightly increased absorbance at ~460 nm as compared to any of the other proteins shown in Figure 2.

EPR Spectra. The EPR spectra of AZPC, PCAZ, AZ, and PC are shown in Figure 3, and the parameters determined from simulations (see Figures S1 and S2) are listed in Table 2. The largest effect of the AZPC loop mutation is to lower g_z and increase A_z as compared to AZ, giving values for these parameters more like those found in PC. The influence of the PCAZ mutation on the EPR spectrum of PC does not really make it more AZ-like, except for the decrease in A_z. The separation between g_x and g_y increases slightly in PCAZ, giving a slightly more rhombic EPR spectrum than that of PC (the EPR spectrum of AZPC is more axial than that of AZ).

Reduction Potentials and the Influence of pH. AZPC yields good quasi-reversible responses on a modified gold electrode in the pH range 3.6−8.1. In most cases, the anodic and cathodic peaks are of equal intensity, and their separation is typically ~60 mV at a scan rate of ~20 mV/s (the peak separation increases slightly as the pH is decreased). The peak currents are proportional to (scan rate)$^{1/2}$ in the range 10−200 mV/s. The E_m of AZPC at pH 7.5 is 362 mV, which is much larger than the value for AZ and is very close to that for PC (see Table 2). In the case of PCAZ, reliable cyclic voltammograms (CVs) could not be obtained on a modified gold working electrode and a PGE was used. The response on this electrode was not ideal, but CVs in which the anodic and cathodic peaks were approximately of equal intensity with separations of 60−90 mV (at scans rates of ~20 mV/s) could be obtained. The E_m of PCAZ at pH 7.5 is 392 mV, which is slightly higher than the value for PC (see Table 2).

The E_m values of both AZPC and PCAZ increase significantly with decreasing pH below ~5 for the former and ~6 for the latter (see Figure 4). The slope of this dependence is ~ −60 mV/pH unit for AZPC (below pH ~ 4.5), and the data for PCAZ are very similar to those for PC down to pH 4.4 (data for PCAZ could not be obtained at lower pH values, and thus the region of this plot with a slope of ~ −60 mV/pH unit could not be accessed). This effect is also observed below pH ~ 5 in PC (~ −60 mV/pH unit slope below pH 4, see Figure 4)[21] and is due to the dissociation and protonation of the C-terminal His87 ligand in the reduced protein.[31] This has a dramatic effect on E_m as the resulting three-coordinate geometry favors the cuprous form. The C-terminal His ligand of AZPC must therefore protonate and dissociate from the Cu(I) site, and we presume the same is also true for PCAZ. The pH dependence of the E_m of PCAZ can be fit to eq 1 giving a pK_a of 4.7 (see Figure S3) for His89 in the Cu(I) protein. For AZPC, the difference in the E_m to AZ, in the pH range 6.5−3.6, gives a pK_a of 4.3 (see Figure S4) for His115. In AZ, the effects observed in the pH 6−8 range are due to the protonation/deprotonation of the noncoordinated His35 and His83 residues whose pK_a values are similar in AZPC and AZ.[32]

$$E_m\,(\mathrm{pH}) = E_m\,(\text{high pH}) + RT/nF\,\ln(1 + [H^+]/K_a^{red}) \qquad (1)$$

Paramagnetic ^{1}H NMR Spectrum of Cu(II) AZPC. The paramagnetic ^{1}H NMR spectrum of Cu(II) AZPC is compared to those of AZ, PC, AZAMI, and AZAMI-F (loop sequence $C^{112}TPH^{115}PM^{117}$) in Figure S5.[9,17,33,34] The experiments in which signals a/b, g, and h in the spectrum of Cu(II) AZPC were irradiated are shown in Figure S6, and all of the assignments made are listed in Table S1 (along with the corresponding data for the proteins included in Figure S5 and also for AMI). The main difference with respect to AZ is the enhanced shift of one of the $C^{\gamma}H$ proton resonances from the axial Met120 ligand. Similar changes are observed in the spectra of AZAMI and AZAMI-F.[9,17]

^{1}H NMR Spectrum of Cu(I) AZPC. In Cu(I) AZPC, the His ligand resonances (the positions of the imidazole ring signals could be identified from the saturation transfer experiments) are not well resolved in the 1D ^{1}H NMR spectrum and broaden considerably at pH values <7.5. Numerous active site resonances are observed in WEFT spectra of partially oxidized samples of AZPC. These resonances are found in positions similar to those in AZ[35] {for example, the His ligand signals and the $C^{\epsilon}H_3$ resonance of the axial Met ligand [found at 0.11 ppm in Cu(I) AZPC as compared to −0.05 ppm in reduced AZ]}. Resonances from the residues giving rise to the upfield shifted signals in the spectrum of the Cu(I) protein (for example,

(28) Jeuken, L. J. C.; van Vliet, P.; Verbeet, M. P.; Camba, R.; McEvoy, J. P.; Armstrong, F. A.; Canters, G. W. *J. Am. Chem. Soc.* **2000**, *122*, 12186−12194.
(29) Lommen, A.; Canters, G. W. *J. Biol. Chem.* **1990**, *265*, 2768−2774.
(30) Groeneveld, C. M.; Canters, G. W. *J. Biol. Chem.* **1985**, *153*, 559−564.
(31) Guss, J. M.; Harrowell, P. R.; Murata, M.; Norris, V. A.; Freeman, H. C. *J. Mol. Biol.* **1986**, *192*, 361−387.
(32) Jeuken, L. J. C.; Wisson, L. J.; Armstrong, F. A. *Inorg. Chim. Acta* **2002**, *331*, 216−223.
(33) Bertini, I.; Ciurli, S.; Dikiy, A.; Gasanov, R.; Luchinat, C.; Martini, G.; Safarov, N. *J. Am. Chem. Soc.* **1999**, *121*, 2037−2046.
(34) Bertini, I.; Fernández, C. O.; Karlsson, B. G.; Leckner, J.; Luchinat, C.; Malmström, B. G.; Nersissian, A. M.; Pierattelli, R.; Shipp, E.; Valentine, J. S.; Vila, A. J. *J. Am. Chem. Soc.* **2000**, *122*, 3701−3707.
(35) van de Kamp, M.; Canters, G. W.; Wijmenga, S. S.; Lommen, A.; Hilbers, C. W.; Nar, H.; Messerschmidt, A.; Huber, R. *Biochemistry* **1992**, *31*, 10195−10207.

Table 2. Properties of AZPC and PCAZ As Compared to Those of the Corresponding Wild-Type Cupredoxins[a]

parameter	AZPC	AZ	PCAZ	PC	AZAMI[a]	AMI[a]
UV/vis[b]						
λ_{max1} [nm]	460(sh)[c]	460(sh)[c]	460	460	470(sh)[c]	460
λ_{max2} [nm]	608	628	608	598	609	596
$\epsilon_{\sim 600}$ [mM^{-1} cm^{-1}]	4.7	5.1	4.9	4.4	4.5	3.9
$A_{\sim 460}/A_{\sim 600}$	0.08	0.07	0.14	0.11	0.07	0.11
EPR[d]						
g_x	2.039	2.035	2.028	2.035	2.033	2.032
g_y	2.049	2.054	2.051	2.044	2.048	2.047
g_z	2.245	2.261	2.233	2.233	2.225	2.235
A_x [mT]	1.0	1.4	6.0	0.5	1.1	0.6
A_y [mT]	0.4	1.4	0.0	0.8	1.0	0.8
A_z [mT]	6.2	5.3	4.8	6.0	6.9	5.4
other						
pK_a^{red} (CV)[e]	4.3	<2[f]	4.7		5.5	6.4[g]
pK_a^{red} (NMR)[h]				4.9[i]		6.7[j]
E_m [mV] (CV)[k]	362	295	392	378	261	255
k_{ese} [M^{-1} s^{-1}][l]	6.0×10^4	2.0×10^6		2.5×10^3	5.5×10^5	1.3×10^5 [m]

[a] Data for AZAMI and AMI are also included and are taken from ref 17. [b] Measured in 20 mM Tris (10 mM phosphate for AZ, AZAMI, and AMI) pH 8.0 (25 °C). [c] Shoulder. [d] Recorded at −196 °C in 25 mM Hepes at pH 7.6 plus 40% glycerol. All of the EPR parameters were derived from simulations using the program SIMFONIA (Bruker). [e] For the C-terminal His ligand in the Cu(I) proteins as obtained from the pH dependence of E_m measured (22 ± 1 °C) by cyclic voltammetry (CV) at $I = 0.10$ M. [f] Estimated value for Cu(I) AZ.[28] [g] Taken from ref 21. [h] For the C-terminal His ligand in the Cu(I) protein determined by NMR spectroscopy. [i] Taken from ref 17. [j] Taken from ref 29. [k] Measured at pH 7.5 (22 ± 1 °C) with the values for AZ, PC, and AZAMI taken from ref 17 and AMI from ref 21. [l] Electron self-exchange rate constant (k_{ese}) measured at 40 °C and in 20 mM phosphate pH* 8.0 for AZ[30] and AZPC and at 25 °C and in 35 mM phosphate pH* 8.0 ($I = 0.10$ M) for PC.[19] The k_{ese} of AZAMI was determined in 20 mM phosphate pH* 8.2 at 25 °C,[17] and the value for AZ at this temperature is 7×10^5 M^{-1} s^{-1}.[30] [m] Measured at 25 °C in 20 mM phosphate pH* 8.2.[29]

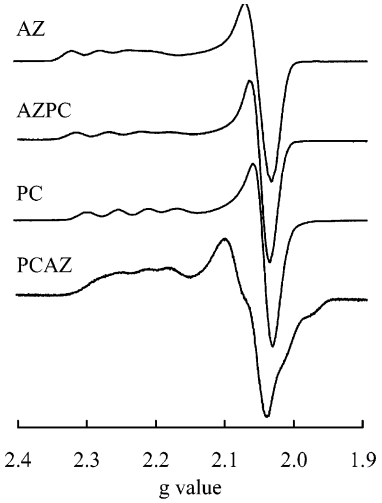

Figure 3. EPR spectra of Cu(II) AZPC and PCAZ as compared to those of AZ and PC at −196 °C in 25 mM Hepes pH 7.6 (40% glycerol).

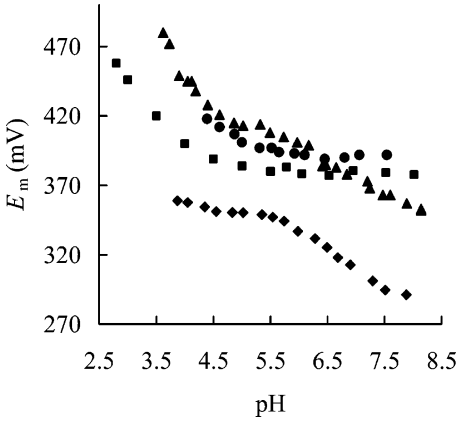

Figure 4. Dependence on pH ($I = 0.10$ M, NaCl) of the reduction potential (E_m) of AZPC (▲), PCAZ (●), AZ (◆), and PC (■).[21] All of the values are referenced to the NHE at 22 °C.

the side chain proton signals of Val22 and Val31) are also found in very similar positions in AZPC and AZ.[35]

ESE Reactivity of AZPC. The electron self-exchange (ESE) rate constant (k_{ese}) of AZPC has been determined at 40 °C using ^{1}H NMR spectroscopy. The influence of oxidized protein concentration on the T_2^{-1} values of active site resonances arising from the Cu(I) protein in the WEFT spectra has been analyzed (see Figure 5), yielding k_{ese} values ranging from 5.1×10^4 to 7.3×10^4 M^{-1} s^{-1}. The average k_{ese} value is 6.0×10^4 M^{-1} s^{-1}, which is confirmed by the coalescence behavior of the Val31 $C^{\gamma}H_3$ resonance in a 1:1 mixture of Cu(II) and Cu(I) protein. Under comparable conditions (40 °C, pH 9.0), k_{ese} for AZ is 2.0×10^6 M^{-1} s^{-1} (see Table 2).[30]

Crystal Structure of Cu(II) AZPC. AZPC crystallizes as a homodimer in which the monomers align via the hydrophobic patch, which surrounds the exposed His115 ligand with a combined buried water-accessible surface area of ∼860 Å^2 (see Table S2). This hydrophobic interface (64% nonpolar atoms) is similar to the monomer contact surface found in the structure of AZ (see Table S2), although the latter is less polar.[4] All of the chimeric cupredoxins that have had their structures determined to date interact through this region within the crystals, although the relative orientation of the monomers is different in each case. In AZPC, the arrangement of the monomers results in an increased Cu−Cu separation (15.8 Å) as compared to AZ (14.9 Å). The rmsd for all equivalent C^{α} atoms between the two monomers of Cu(II) AZPC is 0.29 Å. The overall structure of the Cu(II) protein is very similar to that of oxidized AZ with 118 equivalent C^{α} atoms that superimpose with rmsds of 0.43 Å (using 4AZU, chain A[4]) and 0.46 Å (using 1JZF[5]). The 8 β-strands of AZPC exhibit the highest structural similarity to the AZ structure, while the biggest backbone changes occur in surface-exposed regions. The largest difference is in the ligand-containing loop, which has been mutated from C^{112}TFPGH^{117}-SALM^{121} in AZ to C^{112}SPH^{115}QGAGM^{120} in AZPC, whose backbone adopts a conformation (see Figure 6) identical to that found in PC, the protein whose loop has been introduced (rmsd of 0.27 Å for the C^{α} atoms in the loop).[6,7] This conservation in

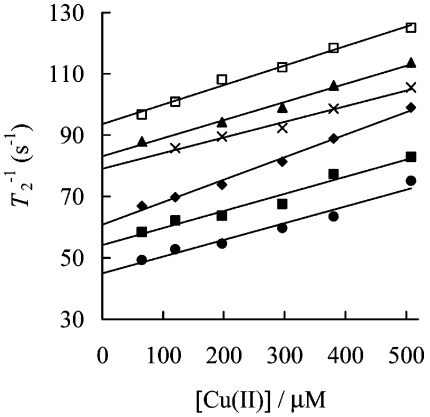

Figure 5. Plots (40 °C) of T_2^{-1} against [Cu(II)] for the signals at 6.05 (●, His ligand $C^{\delta 2}H$ resonance), 0.11 (■, Met120 $C^{\epsilon}H_3$ signal), 10.55 (◆), 7.65 (×), 8.66 (▲), and 9.94 (□) ppm in the WEFT spectrum of Cu(I) AZPC in 20 mM phosphate (99.9% D_2O) at pH* 8.0. Self-exchange rate constants (k_{ese} values) were obtained using the following equation (which is valid for protons belonging to the slow exchange regime); $T_{2,obs}^{-1} = T_{2,red}^{-1} + k_{ese}$ [Cu(II)], where $T_{2,obs}^{-1}$ is the observed transverse relaxation rate of a resonance, $T_{2,red}^{-1}$ is the observed relaxation rate in the fully reduced protein, and [Cu(II)] is the concentration of oxidized protein.

the structures of the loops also applies to the side chains including the ligands (vide infra), with the only exception being an altered conformation for the Gln residue. In PC, the side chain of Gln88 forms an amide−π interaction with the phenol ring of Tyr83.[6,7] This interaction is not possible in AZPC as residues Met56 and Val60 (present on the α-helix found in this region of AZ but not PC) pack to form a hydrophobic interaction with Phe111 (the structural equivalent of Tyr83). The side chain of Gln88 rotates to face the bulk solvent. The mutated loop exhibits small variations between the A and B chains of AZPC that likely arise from different crystal contacts made by Gln12, which change the conformation of its side chain. This alteration is transmitted to Met13, which results in a small shift in the position of the coordinating His115 and influences the conformation of the Met120 ligand (vide infra). Also, the backbone region from 116 to 120 shifts slightly, probably due to the inherent flexibility of the Gln−Gly−Ala−Gly sequence. In AZ, the loop sequence from His117 to Met121 forms a single turn of α-helix,[4,5,10] which is no longer present in the extended His115 to Met120 sequence of AZPC. The hydrogen-bonding pattern involving residues in the loop is different in AZPC as compared to AZ[4,5,10] and almost exactly matches the arrangement found in PC (see Table S3).[6,7] A key hydrogen bond removed by making the AZ to PC loop swap is that between the backbone NH of Phe114 and the coordinating thiolate of

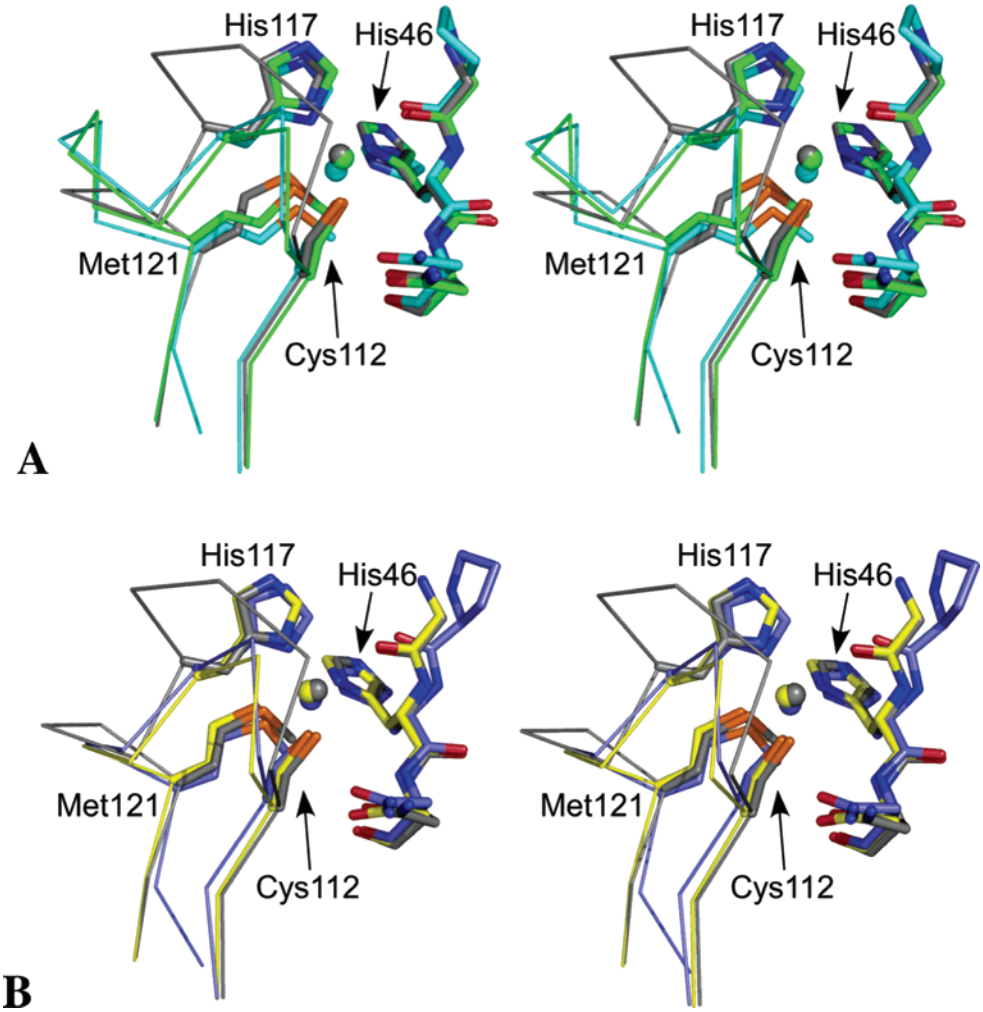

Figure 6. Stereoviews (prepared with Pymol) showing (A) an overlay of the active sites of Cu(II) AZPC (chain A, green), AZ (4AZU,[4] chain A, gray), and PC (1AG6,[6] cyan) and (B) AZAMI (2FTA,[9] chain A, yellow), AZ (gray), and AMI (1AAC,[8] slate). The side chains of the coordinating residues (labeled as in AZ) and the amino acid on either side of the N-terminal His ligand are shown as stick models, copper atoms as spheres, and the backbone of the C-terminal ligand-containing loops as C^{α} traces.

Cys112, as Pro114 (in AZPC) cannot form this interaction. This hydrogen bond is also removed in the AZAMI and AZAMI-F loop contraction variants[9] and also in Phe114Pro AZ.[36] The replacement of the bulky phenyl group of Phe114 situated close to the active site, which is in van der Waals contact with the His117 ligand, is probably responsible for a number of other changes around the active site (vide infra).[9,36]

Other loops adjacent to the copper site are also altered by the AZPC loop mutation. The Gly9 to Phe15, Pro36 to Gly45, and the Met64 to Leu70 regions are most affected, and the Phe to Pro swap at position 114 seems to be partially responsible for two of these changes. The side chain of Tyr72 moves toward the gap created by the removal of the phenyl group, and the Met64 to Leu70 loop relocates in a similar direction. The Lys41 to Gly45 sequence packs against the other side of Phe114 in AZ, and the removal of the phenyl group probably results in the movement of this region. Analogous alterations are observed in the structure of Phe114Pro AZ[36] and also in the AZAMI and AZAMI-F loop contraction variants.[9]

The replacement of Phe114 with a much less bulky side chain in AZPC also alters the solvent structure in the vicinity of the copper. Four water molecules, which are not present in the AZ structure,[4,5] occupy the space created by the removal of the phenyl group (in chain A). One of these water molecules is only 5.3 Å from the copper and hydrogen bonds to the backbone carbonyl oxygen of Gly45, which provides a weak axial interaction with the copper ion (vide infra). Another water molecule is found in the space vacated by the side chain of Pro115 and hydrogen bonds to the backbone carbonyl of Pro114 (this water is 7.3 Å from the copper). This solvent arrangement is different from that in PC but is similar to those in Phe114Pro AZ[36] and also the AZAMI and AZAMI-F variants.[9] The water arrangement around the copper site is different in chain B, due to crystal contacts in the asymmetric unit. The exposed imidazole ring of the His115 ligand is in a slightly different position from that found for His117 in AZ[4,5] due to a small conformational change in its side chain (probably as a consequence of the removal of the phenyl ring at position 114), but still hydrogen bonds to a water molecule that bridges with the backbone carbonyl O of Val43. The solvent accessibility of the active site (ligands) is greater in AZPC than in AZ (see Table S2).

The only significant differences at the Cu(II) site of AZPC as compared to AZ are a lengthening of the Cu−O(Gly45) distance (0.17 and 0.54 Å as compared to 4AZU and 1JZF, respectively, see Table S4) and a slight increase (0.1−0.2 Å) in the displacement of the metal ion from the His_2Cys plane (see Figure 6 and Table S4).[4,5,10] This is despite the removal of one of the two hydrogen bonds to the coordinating thiolate of Cys112 (perhaps slightly compensated by the introduction of a weak hydrogen bond from the backbone NH of the His115 ligand, which is not present in AZ[4,5,10] but is found in PC,[6,7] see Table S3). These changes make the Cu(II) geometry in AZPC slightly more like the distorted tetrahedral arrangement found at the active site of PC,[6,7] but it is still best described as trigonal bipyramidal (like the active site of AZ). An interesting active site change upon introducing the PC loop into AZ occurs at the axial Met120 ligand. In chain A, the Met side chain adopts an all-trans conformation at $C^{\alpha}-C^{\beta}$ (torsion angle χ_1) and $C^{\gamma}-S^{\delta}$ (χ_3) as compared to the gauche arrangement for these angles found in AZ.[4,5,10,37] This matches exactly the conformation of the axial Met92 ligand in PC (see Figure 6).[6,7] In chain B of the AZPC structure, the Met has the same conformation as in AZ. This difference between the A and B chains of AZPC is linked to the subtle changes in the vicinity of the active site, which seem to originate from the altered crystal contacts of Gln12 (vide supra). The intrinsic flexibility of the ligand-containing loop sequence Gly117−Ala118−Gly119, which immediately precedes Met120, may be instrumental in allowing this reorientation. The altered conformation of the axial Met120 in the A and B chains has almost no effect on the geometry of the active site (see Table S4).

There are very few changes at the active site of AZPC upon reduction at pH 5, except for small increases in bond lengths due to the larger ionic radius of Cu(I) (see Tables S4 and S5), which is also the case for AZ[5,38] and AZAMI-F.[9] The axial Met120 ligand is also found in the two different conformations in the A and B chains, which has little influence on the Cu(I) site geometry (see Table S5). As the pH is lowered to 4.0 (data not shown) and 3.5, changes are observed at the active site of Cu(I) AZPC. In particular, the Cu(I)−N(His115) bond starts to lengthen, which seems to be more marked in chain A (see Table S5). This is consistent with the onset of dissociation and protonation of the His115 ligand in the Cu(I) protein as identified by the electrochemistry studies of AZPC. The dissociation and protonation of the His87 ligand of PC on reduction have been structurally characterized in elegant studies at a range of pH values,[31] and a similar effect has been observed for AMI,[39] pseudoazurin (PAZ),[40] and also AZAMI-F.[9] As compared to these other cases, the electron density for the reduced structure of AZPC at pH 3.5 is suggestive of a flip in the histidine side chain (likely to result in a dual conformation in the structure), but at 2.2 Å resolution (the highest obtained for these crystals) it is difficult to confidently assign side chain orientation.

PCAZ was not sufficiently stable to allow crystallization. To try and account for this instability structurally, a model of PCAZ was built by directly grafting the loop from AZ onto the structure of PC with the appropriate residues removed. Visual inspection of this model reveals a possible steric clash involving the side chains of the Thr residue on the AZ loop (Thr113 in AZ adjacent to the Cys ligand which replaces a Ser in PC) and Asn38/Val40 (PC core), and that the adjacent hydrophobic Phe and Pro residues (Phe114 and Pro115 in AZ), which are partly buried in the structure of AZ, are significantly more exposed in AZPC. It is possible that these features destabilize the structure of the loop, which promotes copper loss. It should be noted that PCAMI is a stable chimera[17] and also introduces a Thr in place of Ser adjacent to the Cys84 ligand. However, in PCAMI, the Cys to His sequence is the same length as in PC, whereas in PCAZ this region is extended by two residues.

(36) Yanagisawa, S.; Banfield, M. J.; Dennison, C. *Biochemistry* **2006**, *45*, 8812−8822.
(37) Guss, J. M.; Merritt, E. A.; Phizackerely, R. P.; Freeman, H. C. *J. Mol. Biol.* **1996**, *262*, 686−705.
(38) Shepard, W. E. B.; Anderson, B. F.; Lewandoski, D. A.; Norris, G. E.; Baker, E. N. *J. Am. Chem. Soc.* **1990**, *112*, 7817−7819.
(39) Vakoufari, E.; Wilson, K. S.; Petratos, K. *FEBS Lett.* **1994**, *347*, 203−206.
(40) Zhu, Z.; Cunane, L. M.; Chen, Z.; Durley, R. C. E.; Mathews, F. S.; Davidson, V. L. *Biochemistry* **1998**, *37*, 17128−17136.

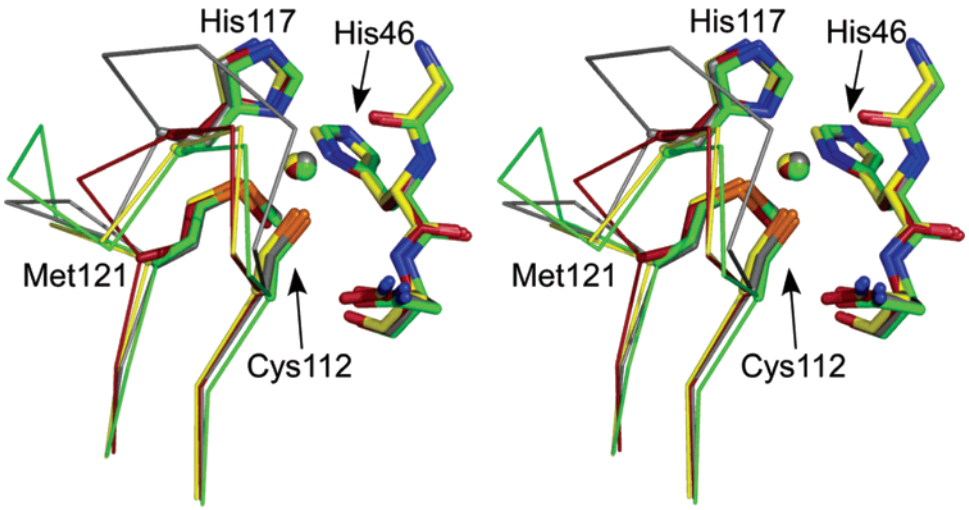

Figure 7. Stereoview (prepared with Pymol) showing an overlay of the active sites of Cu(II) AZ (4AZU,[4] chain A, gray), AZPC (chain A, green), AZAMI (2FTA,[9] chain A, yellow), and AZAMI-F (2FT6,[9] red). The side chains of the ligands (labeled as in AZ) and the amino acid on either side of the N-terminal coordinating His are shown as stick models, copper atoms as spheres, and the backbone of the C-terminal ligand-containing loops as C^{α} traces.

Discussion

Introducing the shorter C-terminal ligand-containing loops of PC and AMI[9,17] into AZ produces stable chimeric cupredoxins. In both cases, the loop adopts structures almost identical to those found in the native proteins (see Figure 6).[6−9] For AZAMI, this is maybe not surprising considering the constraints imposed on the very short loop by the presence of Pro residues either side of the central His ligand. In the case of AZPC, the identical structure of the introduced loop to that of PC is more telling as the His to Met region with the sequence Gln−Gly−Ala−Gly must possess inherent flexibility and is one residue longer than the corresponding region in AZ. It therefore appears that the length and sequence of the copper-binding loop imparts a particular structure around the active site, which can regulate key properties of a cupredoxin. Along with the AZAMI-F mutant (loop sequence CTPHPM), which is smaller than any naturally occurring T1 copper-binding loop,[9] a range of structurally characterized AZ variants are available in which this region has been progressively shortened (see Figure 7). The altered properties of these chimeric proteins cannot be attributed to gross changes in the geometry of the copper center (see Figure 7 and Table S4), and these variants therefore provide an insight into factors outside of the coordinating residues, which can tune T1 site properties.

The spectroscopic properties of AZPC are analogous to those for AZ, which is consistent with their very similar Cu(II) site structures. In the paramagnetic NMR spectrum, one of the $C^{\gamma}H$ proton resonances from the Met120 ligand experiences a larger hyperfine shift than in AZ.[34] This is also true for AZAMI[17] and AZAMI-F,[9] and in both cases the axial Met ligand adopts the same gauche arrangement as in AZ,[9] while in the crystal structure of AZPC two conformations of Met120 are observed (which of these is prevalent in solution is not clear). The position and intensity of the main LMCT band in the UV/vis spectrum are similar in AZPC and PCAZ, and in both cases this is distinct from the values for AZ and PC. This would indicate that the factors that influence the UV/vis details are similar in both loop variants. In AZPC, the increased energy of the LMCT band is most likely due to the loss of the second hydrogen bond to the Cys ligand.[36] In PCAZ, this hydrogen bond is probably absent even though a Phe residue has replaced Pro86 providing the backbone amide, which could form this interaction. The EPR spectra of AZPC and AZ are very similar with the increased A_z for the variant consistent with a small increase in spin density on the copper ion, while the slightly smaller g_z value is probably due to the decreased axial interaction with the backbone carbonyl oxygen of Gly45.[36] Minor changes in spin density distribution around the active site of AZPC, as compared to AZ, are in total agreement with the isotropic shifts of ligand resonances in the paramagnetic NMR spectrum. The EPR spectrum of PCAZ shows a number of differences from that of PC including increased separation between g_x and g_y and is reminiscent of that for PAZ, which indicates that in this case the loop mutation has had a more significant effect on the active site structure (the ligand-containing loops of PC and PAZ have different sequences and structures although they are the same length). This slight enhancement in rhombicity is consistent with increased absorbance around 460 nm in the UV/vis spectrum of PCAZ and would tend to indicate a more tetragonally distorted T1 copper site with possibly a shorter axial Cu−S(Met) bond.[41,42] The copper loss and Cys ligand oxidation observed for PCAZ identifies that if the introduced loop cannot adopt a native-like conformation and pack well against the scaffold, the resulting chimera can be unstable. This identifies an important role in stabilizing and protecting the reactive Cu−S(Cys) moiety for the loop−scaffold interaction.[43]

The most striking influence of the AZPC loop mutation is on E_m, which is raised from the value of AZ to match that found in PC. In AZAMI, E_m is lowered to a value almost identical to that of AMI.[17] In AZAMI-F, further loop shortening raises the E_m value back to that of AZ.[9] The active site geometry of AZ is distinct from that in other T1 copper sites, with the presence of a second axial interaction provided by the backbone carbonyl oxygen of Gly45 being the unique feature,[4,5,10] which is thought

(41) LaCroix, L. B.; Shadle, S. E.; Wang, Y.; Averill, B. A.; Hedman, B.; Hodgson, K. O.; Solomon, E. I. *J. Am. Chem. Soc.* **1996**, *118*, 7755−7768.
(42) Solomon, E. I.; Szilagyi, R. K.; DeBeer George, S.; Basumallick, L. *Chem. Rev.* **2004**, *104*, 419−458.
(43) Hellinga, H. W. *J. Am. Chem. Soc.* **1998**, *120*, 10055−10066.

to influence E_m.[12,44] The corresponding group is usually more distant from the copper, although it is only 3.5 Å away in spinach PC[6] (see Table S4). The Cu−O(Gly45) distance is similar in all of the loop variants (in all cases longer than in AZ), and this feature is therefore not the cause of the observed E_m trends [the small increase in the E_m of AZAMI-F, as compared to AZAMI, may be due to the slightly larger Cu−O(Gly45) distance[36] in this variant (see Table S4)[9]]. In AZPC, the axial Met ligand is seen to adopt a conformation (in chain A only), which is different from that found in AZ,[4,5,10] AMI,[8] AZAMI,[9] and AZAMI-F[9] (the conformation of the Met is the same in all of these structures). This conformation is identical to that of the axial Met ligand in PC[6,7] and other T1 copper sites [PAZ,[45] rusticyanin (RST)[46] and the T1 site of green nitrite reductases (NiRs)[47−49]]. The two Met arrangements appear to have similar energies consistent with studies on other T1 copper sites.[49] Given that the distance of the Met from the copper in AZPC is very similar to those observed for AZ,[4,5,10] AZAMI,[9] and AZAMI-F[9], and the limited contribution of this residue to the electronic structure[42] (not the case for the T1 site of green NiRs[41,42,48]), this ligand is probably not responsible for the observed E_m differences. Therefore, the features that result in the E_m values of AZPC and AZAMI matching those of PC and AMI, respectively, do not seem to be based on active site geometry.

Other factors influenced by the loop mutations, which could alter E_m, include solvent effects,[12,50−54] hydrogen bonding around the active site,[10,36,44] alterations to the dipoles in the vicinity of the copper ion (which will be affected by the hydrogen-bonding pattern),[50,51,54] and the flexibility of the loop (entropic factors).[53] The thermodynamics of reduction of T1 copper sites has been found to be dominated by solvent reorganization effects.[52] The solvent arrangements near the active site of AZPC [Cu(II) and Cu(I) forms] and AZAMI are alike (as is also the case in AZAMI-F) and are different from that seen in the structure of AZ. This arrangement is reminiscent of that in the structure of AMI[8] but not PC.[6,7] In all of the AZ loop-contraction variants, a Pro is found in place of Phe114, and these changes are similar to those observed upon making the Phe114Pro mutation (the E_m value of this variant is ∼90 mV lower than that of AZ).[36] The alterations in solvent structure can therefore be mainly attributed to the removal of the bulky phenyl ring at position 114. Given the distinct effects of the AZPC and AZAMI loop mutations on E_m, it would appear that the solvent arrangement seen in the structures of these proteins has little relevance (the solvent structures are dissimilar in the different chains in the structures of AZPC and AZAMI). The solvent accessibilities (see Table S2) of the ligating residues are similar in AZPC and AZAMI and are significantly greater than in AZ, while the ligands in AZAMI-F are even more solvent exposed (from a visual inspection, the copper ion appears to be more exposed, and to a similar extent, in AZPC and AZAMI as compared to AZ with the metal in AZAMI-F more solvent protected than those of AZAMI[9] and AZPC). It would therefore appear that solvent accessibility is not a main determinant of the E_m trends observed. The increases in E_m in loop elongation variants of AMI have been attributed to mainly entropic effects thought to originate from reduction-induced increases in the flexibility of the introduced loop, due to poor packing of the non-native loops against the AMI scaffold.[14,53] Structures are not available for any of these elongation variants, but the structures of the AZ chimeras demonstrate that the loops of PC and AMI can pack well against this cupredoxin scaffold.

The removal of the second hydrogen bond to the Cys112 ligand in AZPC, and also AZAMI,[9] as compared to AZ[4,5,10] would be expected to result in a sizable decrease in E_m due to the fact that the N−H dipole would destabilize Cu(II).[36,44] This hydrogen bond is also missing in PC[6,7] and AMI.[8] Theoretical studies have shown that numerous permanent protein dipoles around the active site have a major influence on E_m and tune down the value for PC as compared to that found for the solvated active site.[51] The same calculations for RST, an acid-stable cupredoxin with the highest known E_m value (∼700 mV), demonstrate that in this case the protein dipoles increase the potential.[51] In both proteins, residues in the loop, including Pro86, Gly89, Ala90, and Gly91 in PC, provide mainly positive contributions to E_m (the magnitude of the loop contribution is similar for PC and RST). Negative effects come from residues predominantly in the β-barrel scaffold. Similar calculations have not been performed for AZ, but it is revealing that the introduction of the PC loop increases the E_m of this protein. Significant loop shortening, which removes a number of dipoles, decreases the E_m to that found in AMI. It would therefore appear that the contribution from dipoles in the loop is a major contributing factor to the E_m of a cupredoxin. The E_m of PCAZ is marginally higher than that for PC, and in this case the introduced loop probably does not pack well against the scaffold and cannot adopt an AZ-like conformation.

The intrinsic ET reactivity of AZPC, measured using the ESE reaction, is ∼30-fold slower than that of AZ. The reactivity of AZAMI is very similar to that of AZ,[17] while the AZAMI-F variant has a k_{ese} value ∼150-fold smaller than that for AZ.[9] The very small active site changes upon redox interconversion observed for AZPC and also AZAMI-F[9] (at pH values at which His ligand protonation does not occur) highlight that these variations are probably not due to different inner-sphere reorganization energies (which must be comparable to that for AZ[12,55] in all cases). The solvent reorganization energies could have been affected by the mutations, but the magnitude of any alterations is not easily determined[12] and there does not seem to be a simple dependence on loop length. From the structural data, the most likely cause of the altered k_{ese} values are changes in the hydrophobic patch surrounding the exposed His ligand,

(44) Li, H.; Webb, S. P.; Ivanic, J.; Jensen, J. H. *J. Am. Chem. Soc.* **2004**, *126*, 8010−8019.
(45) Inoue, T.; Nishio, N.; Suzuki, S.; Kataoka, K.; Kohzuma, T.; Kai, Y. *J. Biol. Chem.* **1999**, *274*, 17845−17852.
(46) Walter, R. L.; Ealick, S. E.; Friedman, A. M.; Blake, R. C.; Proctor, P.; Shoham, M. *J. Mol. Biol.* **1996**, *263*, 730−751.
(47) Antonyuk, S.; Strange, R. W.; Sawers, G.; Eady, R. R.; Hasnain, S. S. *Proc. Natl. Acad. Sci. U.S.A.* **2005**, *102*, 12041−12046.
(48) Sato, K.; Dennison, C. *Chem. Eur. J.* **2006**, *12*, 6647−6659.
(49) Jacobsen, F.; Guo, H.; Olesen, K.; Ökvist, M.; Neutze, R.; Sjölin, L. *Acta Crystallogr., Sect. D: Biol. Crystallogr.* **2005**, *61*, 1190−1198.
(50) Olsson, M. H. M.; Ryde, U. *J. Biol. Inorg. Chem.* **1999**, *4*, 654−663.
(51) Olsson, M. H. M.; Hong, G.; Warshel, A. *J. Am. Chem. Soc.* **2003**, *125*, 5025−5039.
(52) Battistuzzi, G.; Bellei, M.; Borsari, M.; Canters, G. W.; de Waal, E.; Jeuken, L. J. C.; Renieri, A.; Sola, M. *Biochemistry* **2003**, *42*, 9214−9220.
(53) Battistuzzi, G.; Borsari, M.; Canters, G. W.; di Rocco, G.; de Waal, E.; Arendsen, Y.; Leonardi, A.; Renieri, A.; Sola, M. *Biochemistry* **2005**, *44*, 9944−9949.
(54) Botuyan, M. V.; Toy-Palmer, A.; Chung, J.; Blake, R. C.; Beroza, P.; Case, D. A.; Dyson, H. J. *J. Mol. Biol.* **1996**, *263*, 752−767.
(55) Di Bilio, A. J.; Hill, M. G.; Bonander, N.; Karlsson, B. G.; Villahermosa, R. M.; Malmström, B. G.; Winkler, J. R.; Gray, H. G. *J. Am. Chem. Soc.* **1997**, *119*, 9921−9922.

as this is the recognition surface for the ESE reaction.[56,57] In AZ, large nonpolar residues in the loop make an important contribution to this region,[4,5,10] and the AZPC sequence possesses fewer such side chains (64% nonpolar atoms for the interface involving the region surrounding the C-terminal His ligand as compared to 79% for AZ), with the removal of Phe114 being a significant factor,[36] thus disfavoring homodimer formation. In AZAMI, the introduced Phe117 partly compensates for the loss of the hydrophobic residues, and therefore the k_{ese} value for this variant is almost identical to that of AZ,[9,17] but the removal of this Phe (in AZAMI-F) has a dramatic effect on reactivity.[9] The ligand-binding loop plays an important role in the structure of the hydrophobic patch, which is essential for optimizing a complex structure conducive to fast ET.

The dissociation and protonation of the His ligand in the center of the C-terminal loop is a well-studied characteristic of various cupredoxins[2,20,28,29,31,39,40] and can act as a switch to regulate ET reactivity.[31,58−60] AZ does not exhibit this behavior in the accessible pH range and a pK_a of <2 has been estimated.[28] In Cu(I) AZPC, the pK_a of His115 is 4.3, a value very similar to that for reduced PC[17,21] [the structure of Cu(I) AZPC shows signs that His115 is beginning to protonate at low pH (3.5), but the exact pH values are not easily determined and the crystals could only be soaked under these conditions for very short periods]. In AZAMI, His115 is also seen to protonate in the reduced protein but with a significantly higher pK_a (5.5),[17] reminiscent of that for the His96 ligand of AMI.[21,29] The introduction of the loop structures of AMI and PC into AZ therefore imposes their pK_a values for the His ligand. The pK_a of His89 in PCAZ is probably almost identical to that of His87 in PC. In this case, the introduced loop does not confer its properties on the scaffold protein. However, shortening the active site loop of PC into that of AMI results in the pK_a of the His ligand matching that of AMI (also the case in the PAZAMI variant).[17] A similar outcome as found for PCAZ is obtained when the AZ loop is introduced into AMI (the pK_a matches that of AMI).[53] Analysis of the thermodynamics of dissociation and protonation in this AMIAZ variant has uncovered that the changes in the enthalpic and entropic contributions to this process are opposite (the former increasing the pK_a) as compared to AMI, and overall these cancel.[53] Thus, it would appear that a feature of the loop, which influences the pK_a of the coordinating His, is not reproduced in the PCAZ and AMIAZ variants. Detailed thermodynamic studies of other loop elongation variants of AMI have highlighted that the observed decreases in the pK_a are related to an unidentified entropic feature of the loop. It is interesting to note that the pK_a of the His ligand is 5.9 in AZAMI-F. Thus, in the range of loop contraction variants of AZ (see Figure 7), the pK_a of this residue seems to be related to loop length with a shorter sequence giving rise to a variant with a more readily dissociated His ligand. Detailed thermodynamic studies of these variants are currently underway to shed more light on this matter. It should not be overlooked that all of the loop mutations may have influenced rotational barriers involved in the dissociation and protonation of the C-terminal His ligand,[53] which can have a significant effect on the observed pK_a value.[61] However, a careful analysis of the available data does not identify the structural aspect that could have been altered to affect these processes.

Conclusions

The introduction of shorter naturally occurring ligand-containing loops into AZ gives rise to chimeric cupredoxins in which the structure of this region matches that found in the protein whose loop has been inserted. The active site geometry remains largely unaltered by these sizable changes in the vicinity of the copper. A number of important properties, including the E_m value and the pK_a for the His ligand on the loop, are altered to match the values for the parent proteins. A PC variant into which the longer AZ loop has been introduced is inherently unstable and has features that do not match those of AZ. In this case, the loop probably cannot adopt a native-like structure. The ligand-containing loop is therefore an important structural aspect for fine-tuning a number of functional properties of cupredoxins and for protecting and stabilizing the copper site.

Acknowledgment. We thank BBSRC for funding (BB/C504519). M.J.B. is supported by a Royal Society (U.K.) University Research Fellowship.

Supporting Information Available: Tables showing the ^{1}H NMR data of Cu(II) AZPC and other relevant cupredoxins and loop variants, the interface properties and active site solvent accessibilities of Cu(II) AZPC, AZ, AZAMI, and AZAMI-F, the hydrogen-bonding patterns around the active sites of Cu(II) AZPC, AZ, PC, AZAMI, AZAMI-F, and AMI, and comparisons of the Cu(II) and Cu(I) site geometries of AZPC, AZ, PC, AZAMI, AZAMI-F, and AMI. Also included are figures showing the comparison of the experimental and simulated EPR spectra of AZPC and PCAZ, fits of the pH dependence of E_m for PCAZ and AZPC, the ^{1}H NMR spectra of Cu(II) AZPC as compared to those of AZ, PC, AZAMI, and AZAMI-F, and saturation transfer difference spectra that have been used to assign the ^{1}H NMR spectrum of Cu(II) AZPC. This material is available free of charge via the Internet at http://pubs.acs.org.

JA0661562

(56) van de Kamp, M.; Floris, R.; Hali, F. C.; Canters, G. W. *J. Am. Chem. Soc.* **1990**, *112*, 907−908.
(57) van Amsterdam, I. M. C.; Ubbink, M.; Einsle, O.; Messerschmidt, A.; Merli, A.; Cavazzini, D.; Rossi, G. L.; Canters, G. W. *Nat. Struct. Biol.* **2002**, *9*, 48−52.
(58) Freeman, H. C. In *Coordination Chemistry-21*; Laurent, J. L., Ed.; Pergamon Press: Oxford, 1981; pp 29−51.
(59) Di Bilio, A. J.; Dennison, C.; Gray, H. B.; Ramirez, B. E.; Sykes, A. G.; Winkler, J. R. *J. Am. Chem. Soc.* **1998**, *120*, 7551−7556.
(60) Zhu, Z.; Cunane, L. M.; Chen, Z. W.; Durley, R. C. E.; Mathews, F. S.; Davidson, V. L. *Biochemistry* **1998**, *37*, 17128−17136.
(61) Buning, C.; Comba, P. *Eur. J. Inorg. Chem.* **2000**, 1267−1273.